EXPLICIT INTEGRATION OF BOUNDARY INTEGRAL EQUATIONS AND SCATTERING OF SEISMIC WAVES BY UNDERGROUND STRUCTURES

A. Askar (I)
X. Zeng (II)
S. Altay (III)
Presenting Author: A. Askar

SUMMARY

The goal of this article is 1) to present an efficient method for the integration of the boundary integral equations and 2) to apply th preceding method for studying the effect of the surface topographies on underground structures. A stable explicit integration scheme of the boundary integral equations is presented where the computational effort is of the order of constructing the matrix of coefficients and no matrix inversions are involved. The method is applied to studying the interactions between valleys and tunnels.

INTRODUCTION

The goal of this article is 1) to present an efficient method for the integration of the boundary integral equations and 2) to apply the preceding method for studying the effect of the surface topographies on underground structures. The formation is based on the boundary integral equations.

In most earthquake engineering problems, the response of a system is needed at many discrete values of closely spaced frequencies (usually several hundreds, at intervals $\Delta\omega$ of 0.01 sec^{-1}) and over a fairly large range (usually ω=0 to 25 Hz). Whereas for direct solution procedures, calculations at each frequency are independent ones, the proposed method exploits the information contained at preceding frequencies for constructing the solution at new frequencies. More precisely, the solution at a frequency ω is used as the initial guess for the solution at the frequency $\omega+\Delta\omega$ in an iterative process. Hence, by starting at ω=0 where the initial guess of dropping the integral with the unknown is exact, one can proceed to higher frequencies by updating each time the initial guess by the solution at the preceding step. The procedure can thus be termed as an explicit integration in the frequency domain. Recalling that in many applications, earthquake problems in particular, where one calculates responses over a range of frequencies, this very accurate starting value is provided at no extra cost by the calculations at the preceding frequency. Whereas for direct solution methods, calculations at each frequency are independent from others, the proposed method exploits solutions that are necessarily available at preceding frequencies to achieve significant computational efficiency. Results are presented for the scattering of SH waves by concave (valley) topographies and an internal circular tunnel. Various wave numbers and depths are considered. The purpose in considering the various cases is to see whether one can systematize the responses for given geometries and develop intuition for guessing qualitatively the expected response (Fig. 1).

(I) Visiting Professor, Princeton University, Civil Engineering Dept. Princeton, N.J. 08544 (on leave from Bogazici University, Istanbul, Turkey).
(II) Visiting Scholar, Princeton University, Civil Engineering Dept. Princeton, N.J. 08544 (on leave from National Seismological Bureau, Wuhan, P.R.C.)
(III) Graduate Student, Princeton University, Civil Engineering Department

EXPLICIT INTEGRATION IN THE FREQUENCY OF BOUNDARY INTEGRAL EQUATIONS

Here we present schematically the basic idea involved in the iteration. This is an extension of the work presented in References 1-3. Consider the integral representation for the wave amplitude $\underline{u}$ for harmonic waves

$$\underline{u} = \underline{u}_i + \iint_B \underline{\underline{H}}(\underline{x}-\underline{x}') \cdot \underline{u}(\underline{x}') - \underline{\underline{G}}(\underline{x}-\underline{x}')\cdot \underline{t}_n(x')dA! \qquad (1)$$

where $\underline{u}^i$ is the incident wave displacement vector, $\underline{t}_n$, is the stress vector for the total wave, $\underline{\underline{G}}$ is the matrix Green's function for the homogeneous medium, H is the stress tensor associated with $\underline{\underline{G}}$ dotted by the outward unit normal at the point $\underline{x}'$ and B is the boundary of the region. For a full or half space the integral on the infinite sphere or semisphere vanishes by the radiation conditions. For the infinite space, B consists of the boundary of the foundation, while for a half space, B includes also the boundary of the half space.

The kernels H and G are singular as $x' \to x$ for $\underline{x}$ being a point on the boundary. With this in mind, using the well-known results and interpreting the integrals in the sequel by their principal values, for $\underline{x}$ on B we have the integral equation with $\underline{\underline{\alpha}}$ showing the contribution of the singularities:

$$(\underline{\underline{1}}-\underline{\underline{\alpha}}) \cdot \underline{u}(x) = \underline{u}_i(x) + \iint_B \underline{\underline{H}}(x-x')\cdot\underline{u}(x')dA - \iint_B \underline{\underline{G}}(x-x')\cdot\underline{t}_n(x')dA' \qquad (2)$$

To be specific let $\underline{t}_n = \underline{t}_n^{\,o}$ be prescribed on B. In this case (2) is an integral equation for $\underline{u}$.

We consider incident fields $\underline{u}_i$ characterized by a frequency ω or equivalently wave number k. The above integral equation can be solved iteratively at the frequency $\omega+\Delta\omega \equiv (n+1)\Delta\omega$ by using the solution at $\omega=n\Delta\omega$ in the right hand side terms. Putting in the frequency parameters, Eq (2) leads to:

$$(\underline{\underline{1}}-\underline{\underline{\alpha}}) \cdot\underline{u}(\underline{x},\omega+\Delta\omega) = u_i(x;\omega+\Delta\omega)+ \iint_B \underline{\underline{H}}(\underline{x}-\underline{x}';\omega+\Delta\omega)\ (\underline{u}^i(\underline{x}';\omega+\Delta\omega)+u^s(\underline{x}';\omega))dA' + \iint \underline{\underline{G}}(\underline{x}-\underline{x}';\omega+\Delta\omega)\ \underline{t}_n^{\,o}\ (x';\omega+\Delta\omega)dA' \qquad (3)$$

In this case, no equation is left to be solved. Clearly the stability of such a scheme is the crucial test for its usability. Once this has been established, accuracy is determined by how well the integrals are evaluated numerically and how well is $\underline{u}_s(\underline{x}';\omega)$ an approximation to $\underline{u}_s(\underline{x}';\omega+\Delta\omega)$.

CONVERGENCE AND ACCURACY TESTS

This section establishes the convergence of the proposed scheme both analytically and in an example. Figure 2 presents results for SH waves scattered by a circular cavity for which an exact solution is available as an infinite series. The calculations are carried with $\Delta ka = \Delta\omega(a/c) = 0.1$ for ka=0 to 10. It is hence seen that the solutions thus obtained without any matrix inversions are almost exact. An analytical proof of the convergence of the proposed scheme for the case of a circular hole in infinite space is easily obtained. The integral equation for the scattered displacements obtained from the integral representation for the total displacement is

$$u_s(x) = u_i + \frac{1}{4} \int_0^{2\pi} H_1(2ka \sin \frac{\theta'-\theta}{2}) \ 2ka \sin \frac{\theta'-\theta}{2} \ u(\theta') d\theta' \tag{4}$$

Let

$$u_s = \bar{u}_s + e \tag{5}$$

where u_s and $\bar{u}_s$ are respectively the actual numerically calculated and exact values; e is the error contained in the iterative values. Since the incident wave u_i is prescribed, it contains no errors. The stability analysis is based on considering the amplitudes of the Fourier components of the error. An increase or decrease of these from step n to step n+1 provides the criterion for convergence and divergence. With the exact quantities satisfying the exact equation and with the Fourier components of the error as $e_{n+1}=A_{n+1} \exp i\underline{q} \cdot \underset{\sim}{x}$ and $e_n=A_n \exp i\underline{q} \cdot \underset{\sim}{x}$ the growth factor is obtained as:

$$g = \frac{A_{n+1}}{A_n} = \frac{ika}{2} \int_0^{2\pi} H_1(2ka \sin \frac{\theta'-\theta}{2}) \sin \frac{\theta'-\theta}{2} \ e^{i\underset{\sim}{q} \cdot \underset{\sim}{x}'} d\theta' \ . \tag{6}$$

Thus using the Schwartz inequality and the transformation $\frac{\theta'-\theta}{2} = \chi$

$$|g| \leq ka \int_0^{\pi} | H_1 \ (2ka \sin\chi) | \sin\chi \ d\chi \tag{7}$$

The value of the integral being less than one provides a conservative criterion for convergence. For the high frequencies where convergence due to the high oscillations becomes more critical. Using the asymptotic expansion for the Hankel function, we get

$$|g| \leq \sqrt{\frac{ka}{\pi}} \int_0^{\pi} \sin^{\frac{1}{2}} \chi \ d\chi \simeq 0.4 \sqrt{\frac{ka}{\pi}} \tag{8}$$

This gives a very comfortable upper limit for the frequencies as ka≃20. Once the convergence of the scheme is established, the task now is to evaluate the necessary numerical integrals to a desired accuracy. Table 1 and Figure 2 show comparisons with exact results at ka=1,3,5 and 10. The whole set of calculations for figure 2 (the most expensive set) took only 20 cpu units on Princeton University's IBM 3081. It must be realized that the computational effort is only of the order of constructing the discretized equations of an analogous direct solution of the boundary integral equation.

EFFECT OF SURFACE TOPOGRAPHIES ON TUNNELS

Earlier calculations by several authors on valleys and tunnels indicated quite significant changes in responses and the scattered waves with changes in parameters. In the hope of perhaps systematically understanding the effect of surface topographies on tunnels, we present several case studies. The cases considered are with a flat free boundary as well as boundaries containing concave (valley) topography defined as $\frac{1}{2}A(1+\cos\pi x/a)$ with $A = 0.5$ and 1. The incident waves are taken to be horizontal, at 45° and vertical SH waves and several depths are also considered for a circular tunnel. The Green's function has the form $g = G_o(x-x', y-y') + G_o(x-x', y+y')$ such that the integrals along the flat part of the half space boundary vanish. Similarly the incident wave is taken as the free field solution satisfying stress free conditions on a half space with a flat surface. Some results are displayed in Figures 3 and 4. The total computation time for producing these figures of 27 different parameters was 76 CPU units at Princeton University's IBM 3081.

DISCUSSION

The building of intuition for being able to estimate qualitatively the scattering patterns of seismic waves in the present of surface topographies and structures requires the large number of results. The present set of calculations with various parameter studies were aimed at a systematic understanding of the responses with varying parameters. With the limited number of results presented, the only general conclusion is that the interactions are of long range. This is understandable, since waves decay asymptotically as $1/\sqrt{r}$. It is also seen that the surface topography and the tunnel influence each other quite strongly and their collective behavior is quite different from their individual response. The explicit iterative scheme that is presented is shown to be stable both analytically and with examples up to very high values of the nondimensionalized wave number. Since the scheme does not necessitate matrix inversions, the computational cost is of the order of the construction of the algebraic equations in a direct solution of the boundary integral equations.

REFERENCES

(1) L. L. Chu, A. Askar, A. S. Cakmak, Earthqu.Eng. Struct. Dyn. 9, 205 (1981).

(2) L. L. Chu, A. Askar, A. S. Cakmak, Int. J. Earthqu. Eng. Soil Dyn. 1, 59 (1982).

(3) L. L. Chu, A. Askar, A. S. Cakmak, Int. J. Earthqu. Eng. Soil Dyn. 1,102 (1982).

TABLE 1

Error Analysis for Calculations of the

Problem in Figure 1

	N=10	N=40	N=10	N=40	N=10	N=40
	Δ ka=0.10		Δ ka=0.25		Δ ka=0.50	
ka=1	0.04	0.04	0.10	0.10	0.26	0.26
ka=2	0.16	0.16	0.15	0.15	0.36	0.36
ka=3	0.06	0.06	0.14	0.14	0.39	0.39
ka=4	0.05	0.05	0.15	0.15	0.43	0.44
ka=5	0.10	0.07	0.18	0.16	0.42	0.43

The values N indicate the number of intervals on the semicircle, Δka is the increments used in the integration in the frequency domain.; The values in the table show the error in the norm defined as $\left(\int | u_{ex} - u|^2 \, d\theta'/2\pi \right)^{\frac{1}{2}}$ for the indicated values of ka. u_{ex} and u are, respectively, the exact infinite series solution and the values obtained by the present scheme.

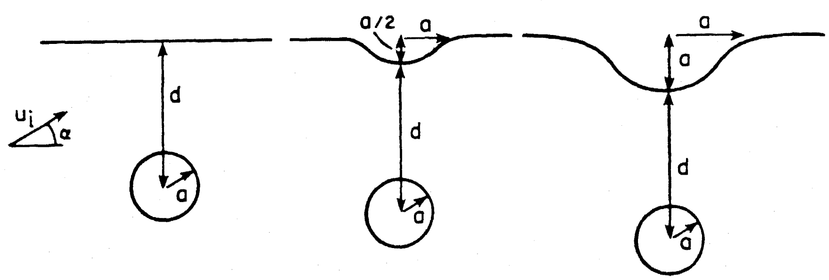

Figure 1: Notation for the Surface Topography, Tunnel and Incident Wave

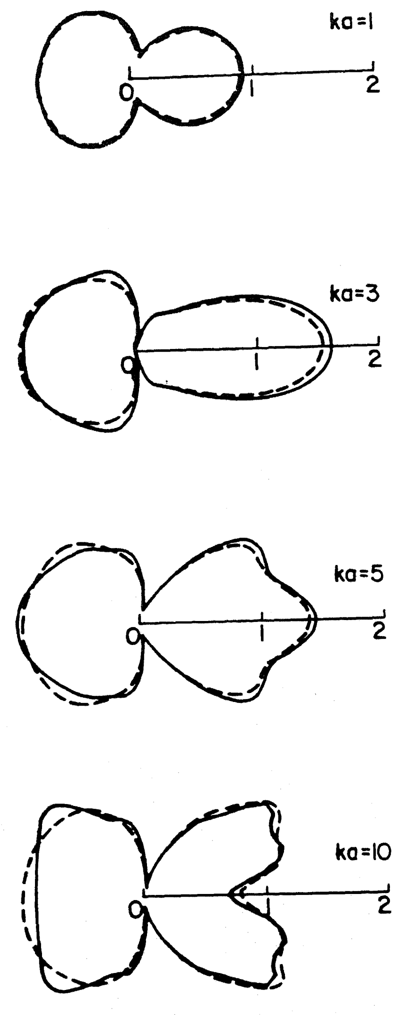

Figure 2: Radial Plots Comparing the Solution by the Present Scheme (—) With That by Exact Infinite Series (---). The Problem is that of a Circular Hole of Radius a with Incident SH-Waves of Wave Number k.

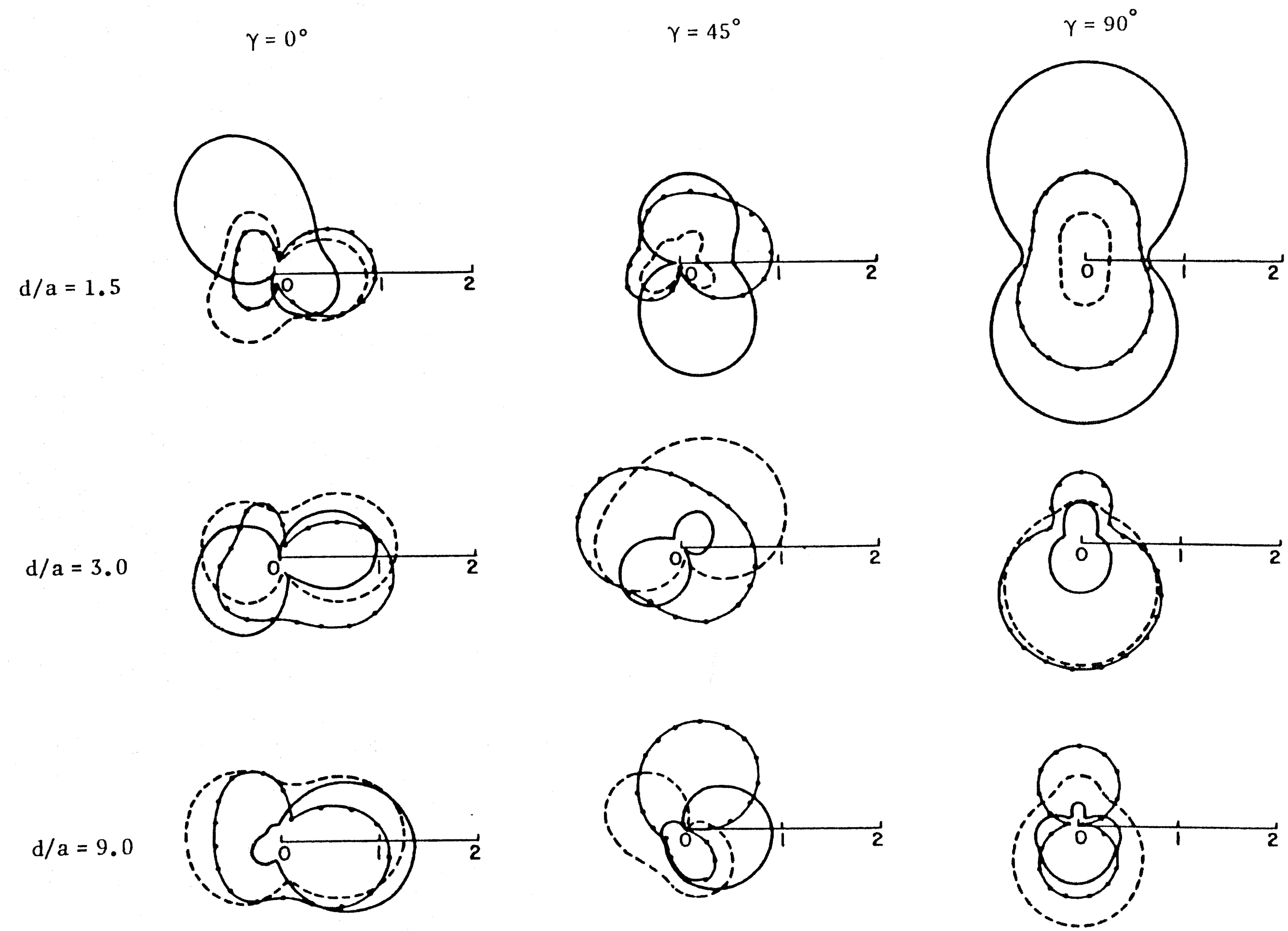

Figure 3: Radial Plots of the Displacement on a Tunnel of Radius a Whose Center is at a Distance d From the Lowest Point on Surface. The Incident Wave Makes an Angle γ With the Horizontal The Free Boundary is Flat (——), or a Valley with Depth $a/2$(---) or a(•••).

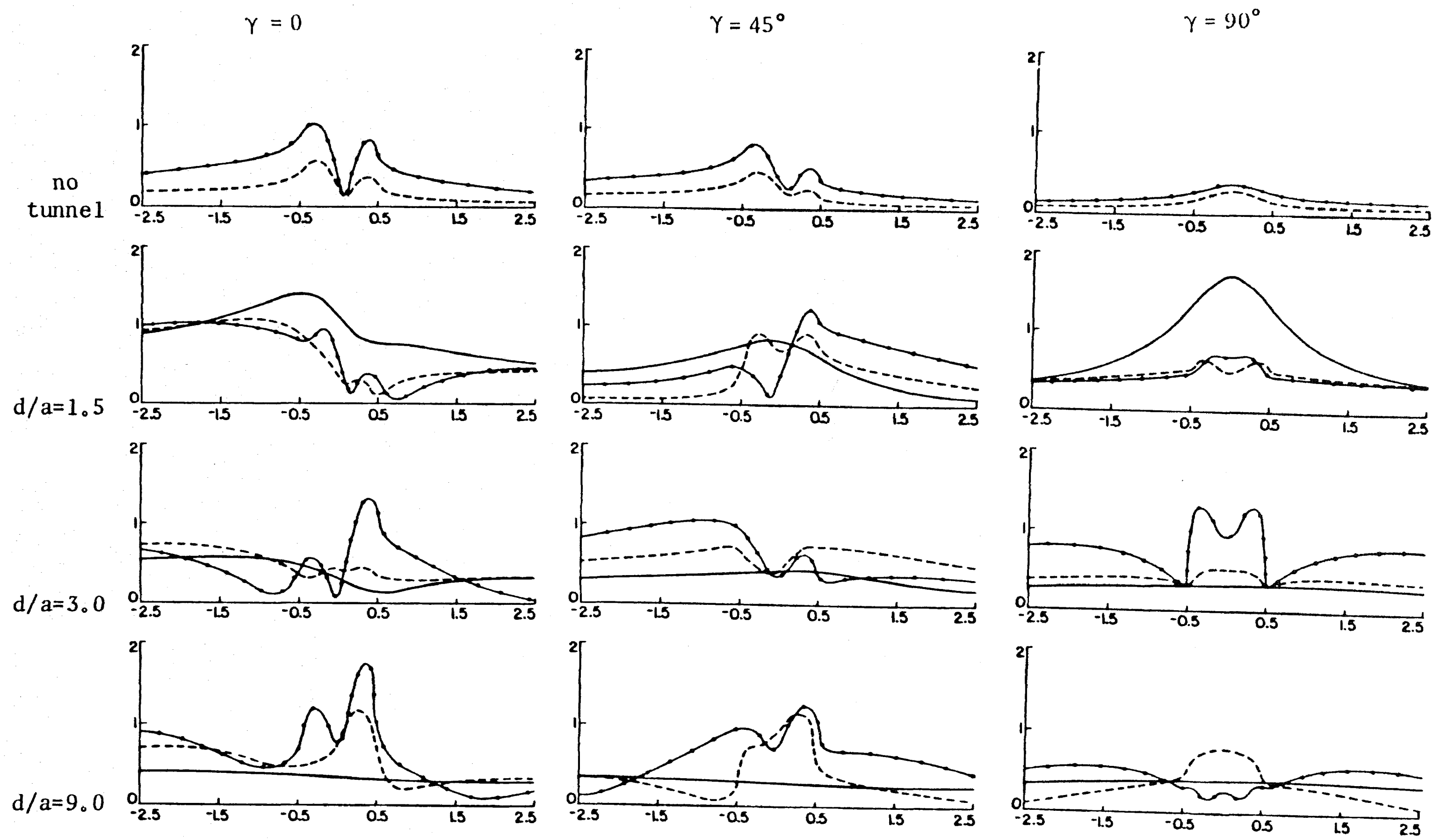

Figure 4: Surface Displacements for the Problem With the Same Parameters as in Fig. 2. The First Plot at Each Angle of Incidence Corresponds to a Case Without a Tunnel (or Equivalently a Tunnel at an Infinite Depth.) The Lines (---), (——) and (-•-•-) Again Indicate, Respectively, a Flat Boundary and Valleys of Depth a/2 and a. The Tunnel Center is at the Distance d from Point 0 on the Horizontal Axis.